AFGL-TR-88-0148

Ionospheric Scintillation Studies

Robert C. Livingston

SRI International
333 Ravenswood Avenue
Menlo Park, CA 94025

1 May 1988

Final Report
October 1984-September 1987

AIR FORCE GEOPHYSICS LABORATORY
AIR FORCE SYSTEMS COMMAND
UNITED STATES AIR FORCE
HANSCOM AIR FORCE BASE, MASSACHUSETTS 01731-5000

Unclassified

SECURITY CLASSIFICATION OF THIS PAGE

REPORT DOCUMENTATION PAGE

1a. REPORT SECURITY CLASSIFICATION Unclassified	1b. RESTRICTIVE MARKINGS
2a. SECURITY CLASSIFICATION AUTHORITY	3. DISTRIBUTION/AVAILABILITY OF REPORT Approved for public release; Distribution Unlimited
2b. DECLASSIFICATION/DOWNGRADING SCHEDULE	
4. PERFORMING ORGANIZATION REPORT NUMBER(S) SRI Project 6674	5. MONITORING ORGANIZATION REPORT NUMBER(S) AFGL-TR-88-0148
6a. NAME OF PERFORMING ORGANIZATION SRI International 6b. OFFICE SYMBOL (if applicable)	7a. NAME OF MONITORING ORGANIZATION Air Force Geophysics Laboratory
6c. ADDRESS (City, State, and ZIP Code) 333 Ravenswood Avenue Menlo Park, California 94025	7b. ADDRESS (City, State, and ZIP Code) Hanscom Air Force Base Massachusetts 01731-5000
8a. NAME OF FUNDING/SPONSORING ORGANIZATION 8b. OFFICE SYMBOL (if applicable)	9. PROCUREMENT INSTRUMENT IDENTIFICATION NUMBER F19628-84-K-0019
8c. ADDRESS (City, State, and ZIP Code)	10. SOURCE OF FUNDING NUMBERS PROGRAM ELEMENT NO. 62101F; PROJECT NO. 4643; TASK NO. 08; WORK UNIT ACCESSION NO. AE
11. TITLE (Include Security Classification) Ionospheric Scintillation Studies	
12. PERSONAL AUTHOR(S) Robert C. Livingston	
13a. TYPE OF REPORT Final	13b. TIME COVERED FROM 10/84 TO 9/87
14. DATE OF REPORT (Year, Month, Day) 1988 May 1	15. PAGE COUNT 44
16. SUPPLEMENTARY NOTATION	

17. COSATI CODES			18. SUBJECT TERMS (Continue on reverse if necessary and identify by block number)
FIELD	GROUP	SUB-GROUP	Radiowave scintillation Ionospheric modification

19. ABSTRACT (Continue on reverse if necessary and identify by block number)

This report briefly summarizes the support provided to AFGL research efforts by SRI International between October, 1983, and December, 1986. This support includes campaign participation, hardware maintenance, software development, data analysis and scientific collaboration.

20. DISTRIBUTION/AVAILABILITY OF ABSTRACT ☒ UNCLASSIFIED/UNLIMITED ☐ SAME AS RPT. ☐ DTIC USERS	21. ABSTRACT SECURITY CLASSIFICATION Unclassified
22a. NAME OF RESPONSIBLE INDIVIDUAL Edward Weber	22b TELEPHONE (Include Area Code) (617) 377-3121 22c. OFFICE SYMBOL AFGL/LIS

DD FORM 1473, 84 MAR

83 APR edition may be used until exhausted.
All other editions are obsolete.

SECURITY CLASSIFICATION OF THIS PAGE

Unclassified

CONTENTS

1. INTRODUCTION 1

Activity Summary 1

A. Support of Long-Term Observation Programs 2

1. Polar Beacon Systems 2

2. HILAT/POLAR BEAR Systems 4

3. Software 5

B. Campaign Support 5

1. December 1983 Campaign 6

2. January-February 1984 Campaign 7

3. January, March 1985 Campaigns 9

4. January 1986 Campaign 9

5. Software 9

6. HILAT Remote Data Access 10

C. Analysis Support 11

1. High latitude Processes 11

2. HF Heater Generated Irregularities 11

3. Spaced Receiver Drift Measurements 12

References 14

Appendix A: Phase Scintillation Measurements During Ionosphere Modification at Arecibo A-1

I INTRODUCTION

The Air Force Geophysics Laboratory and SRI International have collaborated on studies of the ionosphere for many years. This report briefly summarizes the support which SRI has provided to AFGL during the most recent multi-year contract. This support has taken several forms: participation in observation campaigns, hardware maintenance, software support, data analysis and scientific collaboration. The first part of this report briefly enumerates the field support and analysis efforts which were carried out between October, 1983 and December, 1986. Attached as an appendix is a report on one of the scientific analyses performed under the contract.

Activity Summary

Irregular structure in ionospheric plasma density can significantly affect DoD communications and radar systems which utilize transionospheric radiowave paths. An understanding of the production, transport and dissipation of ionospheric structure is therefore of direct relevance to systems currently in use by the Air Force. Furthermore, such an understanding can aid the long-term goal of developing a predictive capability for global ionospheric structure.

Over the past decade, SRI International has assisted AFGL in their studies of the ionosphere, by fielding and maintaining data collection systems, developing software, and collaborating in scientific interpretation. As an innovator in complex signal scintillation theory, measurement and analysis, SRI designed and constructed most of the phase scintillation equipment currently in use for ionospheric research. The HILAT and POLAR BEAR satellite coherent radio beacons were designed and built at SRI, as were the primary ground stations from which those satellite are monitored. Those sites are in Søndre Strømfjord, Greenland, Trømso, Norway, and Churchill, Manitoba, Canada. As a primary contractor for the operation of the satellite ground station and the National Science Foundation incoherent scatter radar in Søndre Strømfjord, Greenland, SRI also provides assistance to a variety of AFGL optical, rocket borne, and radar experiments.

Because of DoD interests, experimental observation of the ionosphere over the past few years has concentrated on high latitudes. This is the most complex portion

of the global ionospheric system; the auroral zone, the polar cap, and the boundary between them can all be regions of highly dynamic and structured plasma. In the polar cap, very large scale plasma patches and sun-aligned arcs occur, and can convect rapidly from their source regions to the entire high latitude region. In the auroral zone, long-term accumulation of particle produced plasma creates high density blobs near the polar cap/auroral oval boundary. Gradients in and around these large ionospheric structures are subject to structuring by convective instabilities, leading to a cascade of energy to short (scintillation-producing) wavelengths. Convective structuring is aided by current-driven instabilities, and the direct imposition of structured plasma concentration by particle precipitation and wave activity. The result is a continuum of irregularities in electron density ranging in spatial scale from hundreds of kilometers to meters or less.

Much of what has been learned about this extended regime of irregularity structure at high latitudes has been through the application of complementary diagnostics: optics, ionosonde, incoherent scatter radar, in-situ satellite, and scintillation measurements. These various techniques allow the observation of structure over several orders of magnitude in spatial scale. The optics, ionosonde and radar provide an overall view of large-scale production and dynamics; the satellites diagnose the inputs to the large- and medium-scale irregularities; from the scintillation data, the strength, shape, and motion of the kilometer-scale structure can be identified. The current AFGL/SRI scientific program is based upon this multi-sensor approach.

During this contract period, SRI involvement in the AFGL scientific program can be roughly divided into three categories of work: (1) hardware, software and analysis support of the long-term observing programs, (2) participation in field campaigns and preliminary analysis of the data collected, and (3) detailed scientific collaboration on selected data sets.

A. Support of Long – Term Observation Programs

1. Polar Beacon Systems

For many years, AFGL has operated a global network of systems continuously

monitoring radiowave intensity scintillation. In 1980, SRI designed and built four systems to extend this capability to the measurement of phase scintillation. The primary advantage of the phase scintillation measurement is that it is a direct indicator of in-situ irregularity characteristics at kilometer spatial wavelengths.

Since the installation of the phase systems, which are currently located in Thule, Greenland, Trømso, Norway and aboard the Airborne Ionospheric observatory (AIO), SRI has been responsible for their maintenance. The AIO system is used only during campaigns, but the ground systems operate continuously, receiving signals from the highly eccentric orbit Polar Beacon satellites. The large volumes of data accumulated by those systems is an important element in defining high-latitude, predictive propagation effects codes. In addition to hardware maintenance, SRI also supports the development and improvement of the codes which are used to process the Polar Beacon data.

During the duration of this contract, several trips were made by an SRI engineer to both Thule and Trømso for purposes of hardware repair of the Polar Beacon systems. The age of the data collection systems has reduced their reliability, and repair in the field is difficult. In the past two years, major failures of both the Thule and Trømso Polar Beacon systems has necessitated their return to SRI for refurbishment. The difficulties have been mostly with the data acquisition systems, but these have been repaired using spare components. The computer terminals and monitoring oscilloscopes built into the systems were also replaced at time of refurbishment. The power supply portions of both receivers were recently rebuilt, and their RF design altered to minimize coherent leakage. All in all, the effort has significantly improved both the reliability and the performance of the rf portion of the systems. At Thule, antennas and preamplifiers have also had to be periodically replaced because of the extreme environment.

Because of the recent difficulties with the data acquisition portion of the Polar Beacon systems, replacement of that part of the system with off-the-shelf hardware has been studied. It was concluded that the replacement costs would be relatively low, thanks to advancements in small computer technology. The upgraded data acquisition system will use a small, general-purpose CPU and operate with a high level programming language. This will make it flexible in application, and capable

of self-diagnosis, which are the two major functional limitations of the original systems. Most importantly, inexpensive board-level spares will be available, and can be installed by field operators. This will minimize the need to send engineering personnel from SRI in response to every system failure.

2. HILAT/POLAR BEAR Systems

Another long-term observing program supported by AFGL involves the DNA HILAT and POLAR BEAR satellites. In 1983, DNA funded SRI to construct and install a ground station for the DNA HILAT satellite at Trømso, Norway. The system is an automatic one, which tracks, records and processes data from several satellite passes each day. Its computer hardware is off-the-shelf, but several other components in the system were custom-built at SRI. Under contract to AFGL, SRI has been responsible for the major hardware maintenance of the station. Between 1983 and 1986, the station operated very successfully, requiring only annual repair trips to replace and adjust receiver signal lock and front end electronics.

In 1986, the possibility of upgrading the HILAT station to simultaneously track the POLAR BEAR satellite was considered. SRI had committed to upgrading the DNA-funded station at Søndre Strømfjord, Greenland for this purpose. Although the POLAR BEAR satellite has fewer instruments than HILAT, it carries a four wavelength scanning imager, with two detectors operating at visual wavelengths, and two operating in the vacuum ultraviolet. The orbit of POLAR BEAR is such that there are many near conjunctions with HILAT. The combination of data in such cases provides much information about auroral E- and lower F-region processes. Another reason to track POLAR BEAR from Trømso is that it greatly expands the image coverage of the polar cap, which would otherwise be limited to single station observations in Greenland. The optical images are of great value in coordinated studies with the EISCAT radar, located only a short distance from Trømso. The round station upgrade plan was accomplished shortly after the POLAR BEAR launch in 1986. The major changes included the replacement of the tracking antenna with a higher gain unit, the addition of a second antenna and receiving system, and the upgrade of the data collection computer and disc system.

3. Software

Both the Polar Beacon and HILAT/POLAR BEAR programs have required continued software support. Processing of the Polar Beacon data to obtain phase is not straightforward because of (among other effects) there are periodic changes in the satellite transmission frequency. This processing is done off-line at AFGL; in conjunction with AFGL data users, several versions of processing software have been developed by SRI for particular applications, and to solve particular problems.

The HILAT and POLAR BEAR data are processed in the field into analysis-ready parameters. However, one of the important parameters which has required off-line calibration is the total electron content (TEC). Absolute TEC is measured in the HILAT and POLAR BEAR systems using the phase dispersion measured over a comb of closely spaced carriers near 413 MHz. However, rf components in the transmitter or receiver can also be dispersive, and this hardware contribution must therefore be carefully measured. This calibration is most readily done using a comparison between radar-measured values of TEC, and those measured by the HILAT system. Early in the HILAT experiment, while making these calibrations, coincident observations of TEC by the EISCAT radar and HILAT showed inconsistencies from pass to pass. These were traced to difficulties in the HILAT TEC algorithm caused by momentary interference and loss of phase lock. Re-analysis of TEC has also been necessary as the receiver front-end system configuration at Trømso has been changed to reduce rf interference.

B. Campaign Support

SRI has participated in AFGL observation campaigns since the installation of phase scintillation systems in 1980. This includes both ground station operations and AIO flights, for which a flight-qualified SRI engineer is available. During this contract, the specific involvement of SRI personnel during observation campaigns has varied with the needs of the observations. During aircraft flights when phase scintillation is a primary measurement, an SRI engineer is on board. During the extended ground measurements, an SRI engineer is usually on site for some period of the campaign, often on a cost-sharing basis with other funding agencies. During

other campaigns when ionospheric or magnetic conditions minimize the scintillation, AFGL has decided that SRI involvement is unnecessary.

1. December, 1983 Campaign

The Defense Nuclear Agency (DNA) HILAT satellite was launched in mid-1983, and was one focus of the December, 1983 high latitude campaign. The purposes of the campaign included (1) coordinate optical and incoherent-scatter radar observations during flights over Søndre Strømfjord, Greenland, (2) obtain coincident optical and scintillation data on the ground and during flights from Thule, Greenland, and (3) obtain aircraft observations in the vicinity of the ionospheric heater near Trømso, Norway, while making comparative scintillation measurements from ground-based receivers. Because of a change in aircraft flight plans, and difficulties with the Trømso heater, the third aspect of the campaign was never implemented, but the first two were very successful.

Prior to the campaign, the AIO receiver was returned to SRI for modification. Normally operated with the Polar Beacon satellites at 250 MHz, the receiver modifications allowed coherent reception of 137 MHz and 413 MHz transmissions from HILAT. Earlier measurements by AFGL engineers had verified that the AIO UHF antenna, although operating near its upper limit, was suitable for use at 413 MHz. Operation at this frequency allowed a relatively simple receiver configuration which utilized much of the existing receiver components. New preamplifier-filters were constructed to allow easy switching between the Polar Beacons and HILAT.

The Søndre Strømfjord radar coordinated flight was carried out under the desired low magnetic activity conditions. Using the Polar Beacon satellite, excellent scintillation data were obtained from the aircraft through optically-observed sun-aligned arcs. As anticipated, the arcs are only weakly structured at intermediate scales, but because of their enhanced electron densities, produce significant phase perturbation at wavelengths of a few kilometers. The radar data, analyzed at SRI, were sent to AFGL where the density distributions and differential plasma velocities could be compared to the optics. These particular comparisons have led to the identification of key features of the physics of polar-cap arc formation.

Following the radar flight, the aircraft systems were operated from the ground at Thule, where a large amount of coordinated optical and scintillation data were obtained. In addition, the ground-based spaced receiver system permanently installed at Thule, was operated in an intensive, continuous observation mode. Virtually all of the observations were under conditions of weak magnetic disturbance and very low polar cap electron densities. This was a result of the rapidly declining solar activity, and provided a distinct comparison with observations at the same season one year before. Because of the lack of ionospheric structure, additional flights from Thule, and those planned to Trømso, were postponed until the January-February, 1984 campaign.

This campaign provided the first opportunity to receive the HILAT satellite beacon signals from the AIO aircraft in flight. The geometry over which useful HILAT signals could be obtained using the aircraft antennas was calculated, and the operation of the on-board data system was confirmed. The experiment pointed out the need for a prompt, on-board satellite position prediction capability, and indicated that further improvements could be made to the HILAT receiver. With the experience gained on these flights, the phase lock bandwidth of the HILAT receiver was narrowed to stabilize lock during weak signal conditions. In addition, in an attempt to minimize the radar interference problems at Thule, a very narrow front end filter was installed in the aircraft. Finally, to optimize scheduling of the HILAT passes, orbital prediction codes were adapted for an SRI desktop computer for use onboard the aircraft.

2. January-February, 1984 Campaign

Ionospheric conditions for the January-February, 1984 campaign were significantly more disturbed than January, 1983. The campaign carried on from that two months earlier, and included extensive ground observations and flights coordinated with other sensors.

One flight from Thule was flown under moderately disturbed conditions. It was designed to characterize the scintillation-producing irregularities in airglow patches using phase scintillation data, and then monitor that structure as the patch drifted

into the field of view of the fixed scintillation receiver at Thule. Overlap between the aircraft optical field-of-view with similar observations from Spitzbergen, Norway, would presumably allow tracking of the large-scale patches from their origins in the cusp into the central polar cap.

Using aircraft position data supplied by AFGL, the relative positions of the radiowave raypaths from the aircraft and the fixed Thule station were calculated. Superimposed on a nominal, two-celled convection pattern, the irregularities sampled early in the aircraft flight would drift through the Thule line-of-sight approximately one hour later. In agreement with the optical data, in which isolated patches could not be identified, the scintillation data from both the aircraft and Thule was nearly uniform in time. The optical homogeneity also precluded confirmation that the raypath did, in fact, remain in approximately the same structured region of the patch. Because of this ambiguity, the detailed comparison of the scintillation measurements was not pursued. The data would provide, however, bounds on the rate of cusp-to-polar cap irregularity decay, and may be pursued in the future.

During the second flight of the campaign, the aircraft path was chosen to optimize coordinated optical observations with HILAT satellite overpasses. During the eight hours of the flight, five near-overhead HILAT passes were recorded. The first of these passes was through a large F-region airglow patch, and saturated intensity scintillation was observed at a radiowave frequency of 137 MHz. The dispersive phase data (equivalent to change in total electron content) shows substructure within the patch as large as a few hundred kilometers. A second HILAT pass intercepted a second optical patch, showing very similar structure. The spectra of the phase data, which can be related to that of the in-situ irregularities producing the scintillation, are similar in form to those seen from fixed polar cap stations. During the most severe scintillation, they are distorted by diffraction effects; during the more moderately disturbed periods, the spectra are two-component power law with a slope break near 300 meters spatial scale. Subsequent HILAT passes were much less disturbed, but provided excellent measurements of the change in TEC associated with quiet E-region arcs.

During the days between the two flights from Thule, several days of scintillation and optical data were collected with the aircraft on the ground. Conditions were

somewhat more disturbed during this period than in December, 1983, providing an interesting morphological comparison. During this time, continuous spaced receiver data were recorded from the fixed Thule ground station.

3. January, March, 1985 campaigns

Two campaigns were carried out in early 1985. The first, in January, was limited to ground observations at Thule. During the second campaign, in March, round robin flights were flown from Thule in support of rocket payloads being launched from Søndre Strømfjord.

Conditions during the January campaign were magnetically quiet; coupled with the low ionospheric electron densities of winter sunspot minimum, very little scintillation was observed. Intensity scintillation at 250 MHz exceeded a level of S4 index greater than 0.3 for only one short period during several days of operations. Because the weak irregularity conditions would undoubtedly extend for several months, it was agreed that SRI should not participate in the March AIO flights. Scintillation conditions were somewhat more interesting in March, but significant structure was observed only in the local afternoon sector. AFGL personnel handled the scintillation observations very capably, and the data were sent to SRI for quick-look analysis to determine particular times of interest. The aircraft receiver and data acquisition system were also returned to SRI to rectify a number of operational problems.

4. January, 1986 campaign

SRI did not participate in the January, 1986 AIO campaign at Thule because of limitations on funding, and the persistence of minimum scintillation conditions in the polar cap. This also allowed postponement of the flight qualification renewal of an SRI engineer. Following the campaigr, some of those data were processed in a quick-look fashion at SRI.

5. Software

Another aspect of data campaign support has been in the development of software required to process aircraft data. Measurement of phase scintillation collected

from a moving platform is much more complex than that from a fixed station. The primary difficulty is that for the Polar Beacon observations, phase is derived from precisely measured changes in source frequency. As such, they include both dispersive (ionospheric TEC and structure) and geometrical (phase path length) components. When the propagation geometry is changing, as on the aircraft, the phase spectrum due to ionospheric irregularities is shifted in frequency, and can be contaminated by geometrical phase changes.

When a stationary signal source is observed from straight-and-level aircraft flight, separation of the ionospheric and geometrical components is simple. At high latitudes, however, the signal sources being used are the Polar Beacon satellites which are in highly eccentric orbits. The geometrical doppler contribution to signal phase is therefore large, and is constantly changing. In addition, the frequency of the beacon aboard the satellite is periodically altered.

During off-line processing, signal phase is reconstructed using changes in frequency measured by the aircraft data receiver. Because of limitations in the computer system, frequency changes are not always reliably recorded. This, plus the removal of large-scale trends in phase caused by deviations in the aircraft flight, make the data reduction time-consuming. This has necessitated a continuing improvement in the processing procedures for the aircraft data; recent adaptation of the procedure to include interactive graphics has significantly simplified the process.

6. HILAT Remote Data Access

Under this contract, support has also been provided to campaigns other than those with the AFGL aircraft. In association with the winter-spring 1985 NASA rocket launches at Søndre Strømfjord, a communications capability between the HILAT and Sondrestrom incoherent radar computers was implemented. This was a cooperative effort, funded by NASA and AFGL, and allowed experimenters at the incoherent radar to see the HILAT in-situ data within minutes of a pass. The system was very simple, yet played an important role in making launch decisions.

Shortly after the rocket campaign, a similar capability was installed by the Canadian NRC at the Churchill, Manitoba, HILAT station. This was used to pro-

vide the same type of near-real time data to experimenters during an auroral electric fields campaign. AFGL then requested that the Trømso, Norway be similarly equipped, so that HILAT data could be available to the Swedish organization in control of the operations of the Viking satellite. A small desktop computer system was purchased for this purpose, and set up to transfer Trømso data to Kiruna, or the nearby Esrange rocket range. The same software used at Søndre Strømfjord were used, with changes required only to operate with the Norwegian modem. While installed in Kiruna, and has played a part in a number of experiments at the Swedish Geophysical Institute.

C. Analysis Support

Periodically, analysis goals for topics of common interest to AFGL and SRI are discussed. Typically, these analyses are concerned with data from previous campaigns.

1. High Latitude Processes

In late January and early February, 1983, a series of coordinated measurements of polar cap arcs and patches was carried out with the AFGL AIO at Thule. Phase screen computations were made for much of the phase scintillation data collected, in order to relate the three-dimensional turbulent strength of the patch and arc irregularities. Scintillation measurements made through distinct patches show that their leading edges are highly structured at kilometer scales, probably by gradient drift processes. Using Sondrestrom incoherent radar observations of patches drifting southward from Thule, and simultaneous optical data from Spitzbergen, it has been possible to track the patches across the entire polar cap. The major findings of the study can be found in Buchau et al. (1985) and Weber et al. (1986).

2. HF Heater Generated Irregularities

Another topic for which the preliminary analysis was recently completed, is the study of irregularities produced by high-power, high-frequency ionospheric heating. Previous experiments of this type have been useful in determining the strength and

decay history of the self-focusing irregularities created by HF heating (Livingston, 1983). In late 1981, AIO flights were flown in the vicinity of the heater facility near Arecibo, Puerto Rico, with a flight path chosen to map the heated volume using a phase scintillation raypath. These data have been analyzed with the results attached as an Appendix to this report.

3. Spaced Receiver Drift Measurements

Another analysis effort pursued under this contract, in cooperation with DNA, was the adaptation of spaced receiver analysis techniques to interpret the data collected by the Polar Beacon systems. A few years ago, a technique originally applied for solar wind drift measurements using radio star sources was successfully adapted to utilize scintillation signals from the polar-orbiting Wideband satellite (Rino and Livingston, 1982). The technique uses analytical expressions which describe the spatial correlation pattern of a received wavefront, as distorted by passage through an irregularity phase screen. The shape of that correlation surface is determined by the irregularity anisotropy, the irregularity drift, and the propagation geometry. Knowing the geometry, the pattern anisotropy and drifts can be extracted from the data in a least-squares sense using the analytical descriptions of the surface. Phase screen model predictions can then be used to imply the in-situ irregularity anisotropy and drift. In practice, it is difficult to obtain high-accuracy drift velocities from the data, but the anisotropy determination has been successful (Livingston et al., 1982).

Adaptation, *per se*, of the spaced receiver phase screen expressions and the data techniques to the Polar Beacon data was straightforward. Although the signal sources have high radial velocities, there is little apparent motion transverse to the raypath. This makes it possible to extract the irregularity drift motion possible in some circumstances. Efforts have concentrated on an explanation of discrepancies between coordinated scintillation- and radar-measured drifts made at Søndre Strømfjord, Greenland. The scalar velocities determined by the two methods are very similar; the scintillation-implied drift direction appears to be dependent upon the propagation geometry.

The conclusion of the work is that there is, at times, distortion of the measured correlation surface which invalidates the generalized quadratic form which the method assumes. If there is any leakage between the temporal (drift) and spatial (anisotropy) contributions to the correlation surface shape, a drift direction bias will be produced. One experimental means to confirm this result, and to possibly obtain a means to further refine the method, is to use simultaneous observations of the Polar Beacon data from Thule and Søndre Strømfjord. Short periods of such coordinated observations were made early in 1983, but weak scintillation conditions make the analysis only marginally useful. A serious experimental effort is being planned for future Greenland campaigns, as the increase in solar activity increases in high latitude scintillation.

REFERENCES

Buchau, J., E. J. Weber, D. N. Anderson, H. C. Carlson, Jr., J. G. Moore, B. W. Reinisch, and R. C. Livingston, "Ionospheric Structures in the Polar Cap: Their Origin and Relation to 250-MHz Scintillation," Radio Sci., 20, 325-338, 1985.

Weber, E. J., J. A. Klobuchar, J. Buchau, H. C. Carlson, Jr., R. C. Livingston, O. de la Beaujardiere, M. McCready, J. G. Moore, and G. J. Bishop, "Polar Cap F Layer Patches: Structure and Dynamics," J. Geophys. Res., 91, 12,121-12,129, 1986.

Livingston, R. C., C. L. Rino, J. Owen, and R. T. Tsunoda, "The Anisotropy of High-Latitude Nighttime F Region Irregularities," J. Geophys. Res., 87, 10519-10526, 1982.

Livingston, R. C., "Heater-Generated Intermediate-Scale Irregularities: Spatial Distribution and Spectral Characteristics," Radio Sci., 18, 253-262, 1983.

Rino, C. L., and R. C. Livingston, "On the Analysis of Spaced-Receiver Measurements of Transionospheric Radio Waves," Radio Sci., 17, 845-854, 1982.

APPENDIX A

Phase Scintillation Measurements During Ionosphere Modification at Arecibo

ABSTRACT

In 1981, a series of flights were made with the AFGL NKC-135 aircraft in conjunction with ionospheric modification experiments at Arecibo. One purpose of the experiment was to estimate the spatial distribution and scale size dependence of thermal self-focusing irregularities produced during heating. This was done using radiowave phase scintillation measured along raypaths in the vicinity of the heated volume to imply the relative strength of heater-generated irregularities. Because phase is an integrated measure of density structure, it is necessary to consider the altitude distribution of irregularities mapped along the magnetic field upward from the heated region toward the F layer peak. The effects of the heating are subtle, but during most of the experiments, an enhancement of irregularity energy is observed in the vicinity of the heater beam. The dependence of thermal self-focusing irregularity wavelength on in-situ heater power density is in agreement with the theory of Cragin et al. (1977).

1 INTRODUCTION

It was predicted many years ago that high frequency radio waves of sufficient energy could alter the temperature of ionospheric plasma. When this heating was first experimentally implemented in the late 1960's, not only was that prediction confirmed, but a whole host of other phenomena were observed (e.g., Utlaut, 1984). Among these effects is the generation of weak electron density irregularities with cross-field widths between a few hundred meters and a few kilometers. The cause of these irregularities is a thermal self-focusing instability (e.g., Farley et al., 1983, and references therein). It arises when small background density variations refract the HF wavefront slightly, focusing the energy into lower density regions, where energy is deposited by ohmic heating; this drives more electrons from the depleted region, and amplifies the thermal and density gradients. The instability grows rapidly until thermal equilibrium is reached, at which point the irregularities are a few percent of the background density in strength. Because there is rapid conduction along the magnetic field, the thermally affected volume (and presumably the irregularity structure) extends well above and below the altitude of heating.

Although the concept of thermal self-focusing is simple, the theory behind it is not. The two working theories which have emerged are those of Perkins and Valeo, (1974) and Cragin et al. (1977). In a comparison of these two theories, Farley et al. (1983) argue that the latter is more likely to be operable under ionospheric conditions. According to the Cragin et al. (1977) theory, the wavelength of the irregularities generated by thermal self-focusing is primarily a function of the HF heating frequency and power density at the heated altitude, with secondary dependencies upon the electron and ion density and temperatures, and plasma scale height. The power density dependence arises from the instability requirement that there be a precise balance between the electron density perturbation which the heating produces, and the dispersive phase effects of that perturbation on the heating signal.

Thermal self focusing irregularities have been observed experimentally using a number of techniques. Farley et al. (1983) made a detailed and unambiguous comparison between observation and theory during one heating event,

using AE-E in situ data and the Arecibo radar. Numerous other incoherent scatter radar observations have been made of specific effects from heating (e.g., Duncan and Behnke, 1978). Because the wavelength of the irregularities is in the kilometer scale regime, it is also possible to use transionospheric radiowave scintillation techniques (e.g., Basu et al., 1983; Livingston, 1983) to observe heating effects. Most of these measurements have been made using intensity scintillation from radio stars or satellites, at propagation geometries which take advantage of the anisotropy of the structure to optimize sensitivity. In the experiment reported here, we use phase scintillation, which is a much more sensitive measure of ionospheric irregularity energy, and makes specific field-aligned propagation geometries unnecessary. But most important, signal phase is a direct, although spatially integrated, measure of density fluctuations along the propagation raypath. At weak scatter levels, and when the irregularities are confined to a limited portion of the raypath, propagation theory shows that the phase power spectrum can be directly related to that of the in situ electron density variations (Rino, 1979). Both of these requirements, weak scatter and thin screen, are satisfied for thermal self-focusing structure generated during heating.

2 EXPERIMENT AND DATA PROCESSING

The data described here were collected during a series of five evening experiments at the Islote, Puerto Rico heater, during September, 1981. Basu et al. (1983) describe the measurements of radio star intensity scintillation during two of these evenings. The phase scintillation data reported here were collected aboard the Air Force Geophysics Laboratory NKC-135 aircraft, using signals from a geostationary satellite. Patterns were flown to the northeast of Arecibo, placing the scintillation raypath to the satellite near, and sometimes through, the heated volume. The experiment was similar to that described by Livingston (1983) in terms of purpose and technique, but was designed to provide a more comprehensive survey of heating-produced structure.

As described in Livingston (1983), the phase scintillation technique used aboard the aircraft can detect very small changes in phase, and is thus sensitive

to both geometrical and dispersive doppler changes in the signal. So long as the aircraft is in straight-and-level flight, as it is during data collection legs of the flight pattern, the geometrical doppler is constant. Removal of this geometrical component leaves the dispersive phase component, proportional to the integrated electron content along the radio raypath. Our interest is in the hundred meter to kilometer scale electron density irregularities, which produce relatively rapid variations in the phase (periods of a few seconds) as they are scanned by the moving raypath.

The phase data are spectrally processed in a conventional fashion to obtain fluctuation energy as a function of frequency. Each spectral sample is derived from 40 s of data, which is long enough to assure stationarity, yet short enough to obtain good spatial resolution. The validity of the phase screen application to heater-generated irregularities makes it straightforward to interpret the computed temporal phase spectrum in terms of the wavelengths of the irregularities which cause the scintillation. The velocity of the propagation raypath through the ionosphere is dominated by aircraft motion, and is essentially constant at 200 m/s. It is this scan velocity, plus or minus the plasma drift, which dictates the spectral frequency-to-wavelength conversion. The background plasma drifts were generally small during the observations; but even during periods of time when the drifts were significant, any velocity-induced offsets are effectively removed by averaging the data from consecutive and adjoining north-south and east-west legs.

The computed power spectrum is that of the naturally-occurring background irregularities, plus a narrow band of enhanced in energy produced the by fixed wavelength heater-generated irregularities. The strength of these enhancements, and the wavelengths at which they occur, provide the basic information we need to determine wavelength dependences and spatial distribution of the heater-generated structure.

3 VERTICAL DISTRIBUTION OF IRREGULARITIES AND PHASE SCINTILLATION GEOMETRY

Low cross-field thermal conductivity limits the horizontal extent of thermal effects during ionospheric modification to the immediate vicinity of the heater beam. Along the magnetic field, however, the thermal conductivity is high, and elevated electron temperatures have been observed at altitudes well above and below the heating altitude (Mantas et al., 1981). The altitude profile of the elevated temperatures is controlled by the loss of electron thermal energy to ions. Above the plasma line (heating) altitude, where the electron density increases rapidly with altitude, the thermal perturbation falls off within 50–75 km; below the heating altitude, the rate of thermal loss is much slower, and the elevated temperatures extend much further downward.

The presence of the thermal pressure gradient over a range of altitudes suggests that electron density irregularities are likely to be present over the same range. It is not clear, however, how the strength of those irregularities might vary with altitude. A first-order assumption might be that the percentage irregularity perturbation, $\frac{\delta N}{N}$, would vary with altitude in the same way as the elevated electron temperature, i.e., it decreases exponentially above the heating altitude, and is nearly constant below. Other processes may have significant effects on the irregularity distribution, however. For example, the polarization electric fields associated with kilometer scale irregularities, which map up and down the field lines with little attenuation (Farley, 1960), might extend the irregularity distribution beyond the region of the elevated temperatures.

The dependence of irregularity strength with altitude is an important factor in the interpretation of the phase scintillation data. Phase scintillation includes the integrated effects of irregularity density structure along the raypath through the ionosphere; unlike a point measurement, contributions to scintillation can come from different altitudes. Furthermore, the phase deviations produced by fluctuations in electron density are proportional to δN^2. As a result, points in the aircraft track where the raypath intercepts the directly heated volume might show less scintillation than raypaths which penetrate

the heated flux tube at higher altitudes where the perturbation percentage is smaller, but the background density is higher. This becomes a problem when the data are to be used to determine the spatial distribution of irregularity strength with respect to the heater beam and heating altitude. In Section 5, a specific distribution of irregularity strength with altitude will be assumed, in order to obtain irregularity maps.

4 IRREGULARITY WAVELENGTH DEPENDENCE

Figure 1 shows the dependence of thermal self-focusing irregularity wavelength on power density and frequency, as predicted by Cragin et al. (1977). A typical nighttime plasma line density of 3.5×10^5 and a scale height of 100 km have been assumed. In Table I we have used this dependence to predict the dominant thermal self-focusing irregularity wavelength for the four evenings of data that will be discussed. The transmitter and antenna configuration are as reported during the experiments; the heater in situ power density was estimated to be 40 $\frac{\mu W}{M^2}$ on day 266, and we have used this value as a reference for the later nights. The rightmost column in Table I is the dominant irregularity wavelength predicted each evening, assuming an unperturbed electron/ion temperature of 900°K. Because of the differences in operating frequency and power levels from evening to evening, the predicted irregularity wavelength ranges from about 500 m to 1050 m. This much of a difference should produce a small, but statistically measurable, change in the phase spectral shape.

Table I

Heater Parameters and Predicted Dominant Thermal Self-Focusing Wavelengths During the Phase Scintillation Observations

Day	Frequency (MHz)	Number of Transmitters	Transmitter Power (kW)	Antenna Configuration	Power Density ($\mu W/m^2$)	Wavelength (m)
266	7.3	3	135	full	55	500
267	5.1	2	100	full	28	920
268	5.1	2	100	half	14	1050
268	5.1	3	100	half	21	1000
269	5.1	3	100	full	42	800

In Figure 2, the overall distributions of observed spectral energy in two wavelength windows (500–800 m and 1250–800 m) are plotted; they have been ordered, top to bottom, according to the predicted irregularity wavelength. All of the data for which the raypath was within about 100 km of the heated volume, are included in the distributions.

The energy units are db rad^2, obtained by integrating over the specified range of each phase power spectrum. In reality, rather than the single dominant wavelength that theory predicts, a range of irregularity wavelengths are likely produced during the heating. The distributions in Figure 2 must reflect that spread, but are also broadened by naturally occurring structure, any secondary structuring of the heating irregularities, and the altitude dependence of irregularity strength.

It can be seen in Figure 2 that there is a shift in energy from shorter wavelengths on days 266 and 269, to longer wavelengths on days 267 and 268, in agreement with

self-focusing theory. At the longer wavelengths, the observable difference is in the maximum energy range of the distributions, rather than their means. This suggests that at these larger scales, there is a consistent background distribution of naturally-occurring irregularities, from which it is difficult to distinguish heater-generated structure. This is not the case at the shorter scales, where the heating structure appears to dominate any natural structure, and the mean phase energy shifts by more than a factor of two between days 266 and 267.

It is difficult to discern any significant difference between the day 266 and day 269 distributions, despite the fact that theory would predict a shift to larger wavelengths on day 269. We note, however, that the observations are easily within the uncertainty of our power density assumptions. In particular, we have assumed that the antenna pattern and efficiency are the same at 5.1 MHz and 7.3 MHz.

Comparing the distributions for the day 267 and day 268 distributions, their means are shifted in the opposite direction expected from the theory. Two factors may explain this discrepancy. One is that the boresite gain of half the antenna field used on day 268 was assumed to be is exactly half that of the full field; a slightly better gain could shift the predicted day 268 wavelengths to shorter scales. The second factor is that, as the spatial maps in Section 5 will show, there is something unusual about the heater antenna pattern on day 267, suggesting that the power density may be significantly lower than shown in Table I.

Figure 2, then, confirms first-order agreement between the wavelength dependence of heater irregularities predicted by Cragin et al. (1977) and our observations. Considering the approximate nature of the power density assumptions, the agreement seems remarkably good.

5 IRREGULARITY SPATIAL DISTRIBUTION

As was pointed out in Section 3, the use of a height-integrated measure of structure, such as phase scintillation, to obtain a spatial distribution of irregularities requires some knowledge of the vertical distribution of density structure. In particular, to reference the phase scintillation strength to the location of the heating beam at the heating altitude, requires assumptions about the strength of the density irregularities along the heated flux tube. Lacking any experimental data or theoretical guidelines

for this altitude dependence, we have assumed that the irregularity structure strength, δN, is constant with altitude between the heating altitude and the F layer peak. Below the heating altitude, it is a good assumption that the electron density is too low to contribute significantly to the scintillation. Above the heating altitude, we know that the thermal perturbation decreases with altitude, but assume that this is counteracted by the rapidly increasing electron density, producing a constant δN. The advantage of this model is its simplicity in handling the data; if reasonable spatial distributions are obtained, it will be a rough confirmation that such a vertical distribution is produced by heating.

In practice, to consolidate the phase energy into a map, a series of penetration altitudes along each raypath (i.e. each spectral sample) are specified between the F layer peak and the heating altitude. The penetration latitudes and longitudes for each altitude are calculated, and are field line traced to the heating altitude. Each spectral sample therefore falls at multiple points in a map grid; the structure energy (assumed to be constant from each altitude, as noted above), is incorporated into the average energy sum at that grid point.

5.1 Day 266, 1981 (September 22-23)

Figure 3 is a map of the geometry of the observations on this evening. One trace is the propagation penetration location at the plasma line altitude, the other is the penetration of the F layer peak mapped down to the plasma line altitude; this illustrates the range of propagation geometries which have been used to account for the vertical mapping of irregularity structure.

This was one of two evenings during which the Arecibo incoherent scatter radar was used to monitor ionospheric density and plasma drifts. Figure 4 summarizes those data, the plasma line (heating) altitude, and the heater schedule. The top frame in Figure 4a shows the typical Arecibo pattern of F layer midnight altitude collapse; coupled with the nearly constant F layer peak density, the midnight collapse caused a progressive steepening of the bottomside plasma scale height, from 100 km to about 25 km. Except for very early in the experiment, plasma drifts were low and disorganized.

Because of the high F layer critical frequency on this night, the heater was operated at 7.3 MHz. Heater power was 400 kW into a full antenna field, and was O-mode. As shown in Table I, the estimated power density at the plasma line height is 55 $\frac{\mu W}{M^2}$,

corresponding to a dominant irregularity wavelength near 500 m; Figure 2 confirms that this wavelength estimate is approximately correct.

Figure 5 shows contour maps of the distribution of irregularity energy in three wavelength ranges. The first wavelength range (2000–1250 m, Figure 5a) should be unaffected by the heating on this and other nights, and any variation reflects the decay and/or large scale spatial variation of ionospheric electron content. The overall variation is relatively small, although there seems to be an east-west gradient and a roll-off in electron density to the southwest. The contour level units are in db [radians^2], as extracted from the phase spectra before averaging and gridding. The second and third contour maps show the distribution of energy in the wavelength ranges which should include the structure generated by thermal self-focusing: 1250–800 m, and 800–500 m. Superimposed on each map is the heater beam main lobe pattern, whose 3 db power point is approximately an ellipse 40 km north-south, and 20 km east-west (Gordon and Dobelman, 1982).

On the 1250–800 m wavelength map (Figure 5b), there is some variation in energy over the the region sampled, but no particular enhancement of energy in the vicinity of the heater beam. At shorter spatial scales, however (Figure 5c), there is a significant enhancement just adjacent to the heater beam. On this same map, there is a rapid fall off of energy to the north of the beam, but a broad fan of structure to the south, only slightly weaker than the peak enhancement. We note that this same asymmetry in energy is seen in the 1250–800 m map; such broadband structure may be naturally occurring ionospheric structure resulting from the unsettled velocities and high F layer density.

5.2 Day 269, 1981 (September 25-26)

The propagation penetration scans for this evening corresponding to the heating altitude and the mapped F layer peak, is shown in Figure 6. During the flight, background ionospheric conditions were monitored by the Arecibo radar. This night was unusual in that the F layer altitude remained high well past midnight, compared to its usual pre-midnight collapse (Figure 4d). Associated with the high layer is a consistent, but slowly decreasing zonal plasma flow throughout the evening. Duncan and Behnke (1978) observed thermal self-focusing structure drifting with the plasma out of the heated volume. If this is the case here, the consistent eastward plasma drift

should produce a downwind trail of structure to the east of the heater beam.

As shown in the bottom panel of Figure 4, the heater operated at 5.1 MHz and a power of 300 kW (400 kW for a short period), into a full antenna field with left circular (O mode) polarization. The estimated in situ power density for most of the evening was 42 $\frac{\mu W}{M^2}$, which should produce irregularities of approximately 800 m wavelength (Table I).

Figure 7 shows the irregularity structure contour maps for day 269. The largest spatial scales show almost no variation in energy, consistent with the nearly constant F layer peak density shown in Figure 4d. The 1250–800 m regime shows some variation over the mapped area, but there is nothing clearly associated with the heater beam. At shorter spatial scales, however (Figure 7c) there is much more variation across the grid and a significant enhancement north of the heater beam. This would suggest that the irregularities are at wavelengths shorter than 800 m, as noted for the distributions in Figure 3. The maximum observed enhancement is to the north of the heater beam, but this could be due, in part, to our simple model of vertical irregularity distribution. If the irregularity strength is not constant with altitude, or if the structure maps above the F layer peak, the contour pattern will shift. We also note that the contours are consistent with a redistribution of the irregularities by bulk plasma drift; the broad region of enhanced structure to the north-north-east of the beam suggests that the heater irregularities have convected out of the heated beam and to the east. More difficult to explain is the broad region of structure that lies to the west of the beam, and is 2–3 dB weaker than the peak enhancement. One possible explanation is that it is naturally occurring structure associated with the large-scale density gradient seen in Figure 7a.

5.3 Day 268, 1981 (September 24-25)

On this evening, the aircraft pattern flown was very similar to that on day 269 (Figure 6). Plasma line height was derived from ionosonde measurements at Arecibo, but no other supporting measurements are available since the Arecibo antenna was being used for radio star scintillation measurements (Basu et al., 1983). In order to obtain an estimate of the irregularity distribution for this experiment, we have assumed an F layer altitude based upon the plasma line height behavior. On the two nights with supporting data (Figure 4a and 4d), the F layer peak/plasma line height

separation ranges from about 100 km at 22 LT to 40–60 km at 02 LT. As shown in Figure 4c, we have assumed a similar pattern for interpretation of this night's data.

One significant difference in the heating this night was that although the heater power was 300 kW, and later 400 kW, only half of the antenna field was being used. This reduces the estimated in situ power density to about half that on day 269. At this power density, 5.1 MHz heating (O-mode) will produce relatively large irregularities, greater than 1000 m wavelength (Table I).

The difference between the irregularities generated this night, compared to the two nights already shown, is obvious in the contour maps in Figure 8. At scale sizes larger than 1250 m, the energy is relatively flat. Similarly unstructured is the energy at scales sizes shorter than 800 m, in distinct contrast to the two nights already discussed. For the 1250–800 m range, in which the predicted 1000 m irregularities should be centered, a strong enhancement is seen just north of the heater beam. The enhancement is more isolated than that seen in the previous maps, suggesting very low plasma drifts, and thus little redistribution of irregularities. An earlier southeastward plasma drift could be postulated as the cause of the structure (−7 db contours) to the southeast. Redistribution seems more likely than the occurrence of natural irregularities since the 800–500 m map shows no corresponding enhancement in the same area.

5.4 Day 268, 1981 (September 23-24)

On this evening, there is approximately an hour of plasma line height data available; after that, a power failure at the ionosonde site precluded any additional measurements. In order to obtain some estimate of the spatial distribution of structure, guesses were made about the plasma line and F layer peak altitudes as shown in Figure 4b.

The heater operated at 5.1 MHz, at a reduced power output of 200 kw, into the full antenna field. As on the other nights, heating was O-mode. As shown in Table I, the estimated irregularity scale produced should be about 920 m, corresponding to an in situ power density of about 28 microwatts/meter squared.

The contour maps for this night are shown in Figure 9. At the largest scales, little structure is seen, other than a rapid roll-off in energy to the far south (Figure 9a).

The contour levels are significantly higher than on the other nights, however, perhaps suggesting high F layer densities. The contour map for the short scales (Figure 9c) indicates only weak structure, consistent with the predicted irregularity wavelength. The 1200–800 m map (Figure 9b), shows what is apparently the predicted 900 m heater-produced structure, but in a very different spatial pattern than expected from the single main lobe of the heater beam. There are two regions of irregularity structure, comparably disturbed, spaced to the northeast and southwest of the heater boresite. If they are significantly in error, the simple model of vertical irregularity distribution and the assumed ionospheric altitudes could both distort the contours. However, as distinct pattern as that seen in Figure 9b may indicate that the heater antenna pattern actually may have been different during the day 267 experiment.

6 SUMMARY

Thermal self-focusing irregularities have cross-field wavelengths between a few hundred meters and a few kilometers. At these scale sizes, the irregularities can be observed using phase scintillation techniques. Weak scatter, thin phase screen propagation assumptions apply to heater-generated structure, which means that the phase spectrum is related directly to the in situ density spectrum. We have taken advantage of this association, and have made observations of phase energy as a function of irregularity wavelength, under different heating conditions. The energy distributions show that the wavelengths of thermal self-focusing irregularities agree well with the theory of Cragin et al. (1977). When the irregularities are larger than 800–900 m, they are difficult to discern in the phase spectra because the naturally-occurring background density fluctuations have comparable energy. At shorter scale sizes, the background fluctuation spectrum rolls off steeply and the presence or absence of heater irregularities at these wavelengths is conspicuous.

One advantage of an airborne experiment is that the mapping of a large area can be obtained; in this case, our purpose was to obtain a spatial map of heater-generated structure relative to the heater beam. This task is complicated by the integrated nature of the phase scintillation measurements, since heater irregularities are produced up and down the magnetic field from the directly heated volume. The upward and downward extent of thermal perturbations during heating have been studied, but the altitude distribution of irregularities, and their variation in strength, has never been modelled

or measured. In order to produce irregularity spatial maps from the phase data, we have assumed that the heating irregularities extend from the heating altitude to the F layer peak, with constant strength over this altitude range. Magnetic field line mapping downward from a series of penetration altitudes along each raypath allows the energy contributions from different altitudes to be consolidated onto a map, and referenced to the heater beam location and heating altitude. This simple model appears to be approximately correct, since the irregularity maps from three of four evenings show enhancements in the vicinity of the heater beam.

The results reported here are observational, and have been presented with a minimum of physical analysis and interpretation. There is much more that could be done with the data. For example, the energy distributions with wavelength and the spatial maps could be improved by a specific removal of modelled background irregularity energy. Probably most useful to a refined analysis would be a theoretical model describing the vertical distribution of thermal self-focusing irregularities. Nevertheless, the results shown here aid in the understanding of thermal self-focusing irregularities and their measurement using phase scintillation techniques.

7 REFERENCES

Basu, S., S. Basu, S. Ganguly and W. E. Gordon, Coordinated study of subkilometer and 3-m irregularities in the F region generated by high-power heating at Arecibo, *J. Geophys. Res.*, *88*, 9217, 1983.

Cragin, B. L., J. A. Fejer and E. Leer, Generation of artificial spread-F by a collisionally coupled purely growing parametric instability, *Radio Sci.*, *12*, 273, 1977.

Duncan, L. M., and R. A. Behnke, Observations of self-focusing electromagnetic waves in the ionosphere, *Phys. Res. Lett.*, *41*, 998, 1978.

Farley, D. T., A theory of electrostatic fields inthe ionosphere at nonpolar geomagnetic latitudes, *J. Geophys. Res.*, *65*, 869, 1960.

Farley, D. T., C. LaHoz and B. G. Fejer, Studies of the self-focusing instability at Arecibo, *J. Geophys. Res.*, *88*, 2093, 1983.

Gordon, W. E., and J. A. Dobelman, Comparison of measured and calculated antenna patterns for Islote heater, report, Rice University, Houston, Texas, 1982.

Livingston, R. C., Heater-generated intermediate-scale irregularities: Spatial distribution and spectral characteristics, *Radio Sci.*, *18*, 253, 1983.

Mantas, G. P., H. C. Carlson and C. H. LaHoz, Thermal response of the F region ionosphere in artificial modification experiments by HF radio Waves, *J. Geophys. Res.*, *86* 561, 1981.

Perkins, F. W., and E. J. Valeo, Thermal self-focusing of electromagnetic waves in plasma, *Phys. Rev. Lett.*, *32*, 1974.

Rino, C. L., A power law phase screen model for ionospheric scintillation studies, 1. Weak scatter, *Radio Sci.*, *14*, 1135, 1979.

Utlaut, W. F., Ionospheric modification induced by high-power HF transmitters- A potential for extended range VHF-UHF communications and plasma physics research, *Proc. IEEE*, *63*, 1022, 1975.

Figure 1. Thermal Self-Focusing Irregularity Wavelength Dependence on in situ HF Power Density, after Cragin et al. (1977). The heating frequencies of 5.1 MHz (solid) and 7.3 MHz (broken) are those used in the experiment. The assumed plasma scale height is 100 km, and the background electron-ion temperatures are as indicated.

Figure 2. Distributions of Phase Energy from two Wavelength Windows for the Four Evenings of Observation. The predicted dominant self-focusing wavelength for each evening is as indicated.

Figure 3. Propagation Raypath Penetration Locations for Day 266, 1981, for the Heating Altitude (solid) and the F Layer Peak Field Line Mapped to the Heating Latitude (broken).

Figure 4. A Summary of Ionospheric Conditions and the Heating Schedule for the Four Evenings of Observation, Day 266 (a), Day 267 (b), Day 268 (c), and Day 269 (d). The dashed altitude lines on days 267 and 268 are estimated only.

Figure 5. Phase Energy Contour Maps for Day 266, 1981, for Three Irregularity Wavelength Windows. The plus sign is the heater location, and the ellipse is the nominal 3 dB heater antenna pattern.

Figure 6. Propagation Raypath Penetration Locations for Day 269, 1981, for the Heating Altitude (solid) and the F Layer Peak Field Line Mapped to the Heating Altitude (broken).

Figure 7. Phase Energy Contour Maps for Day 269, 1981, for Three Irregularity Wavelength Windows.

Figure 8. Phase Energy Contour Maps for Day 268, 1981, for Three Irregularity Wavelength Windows.

Figure 9. Phase Energy Contour Maps for Day 267, 1981, for Three Irregularity Wavelength Windows.

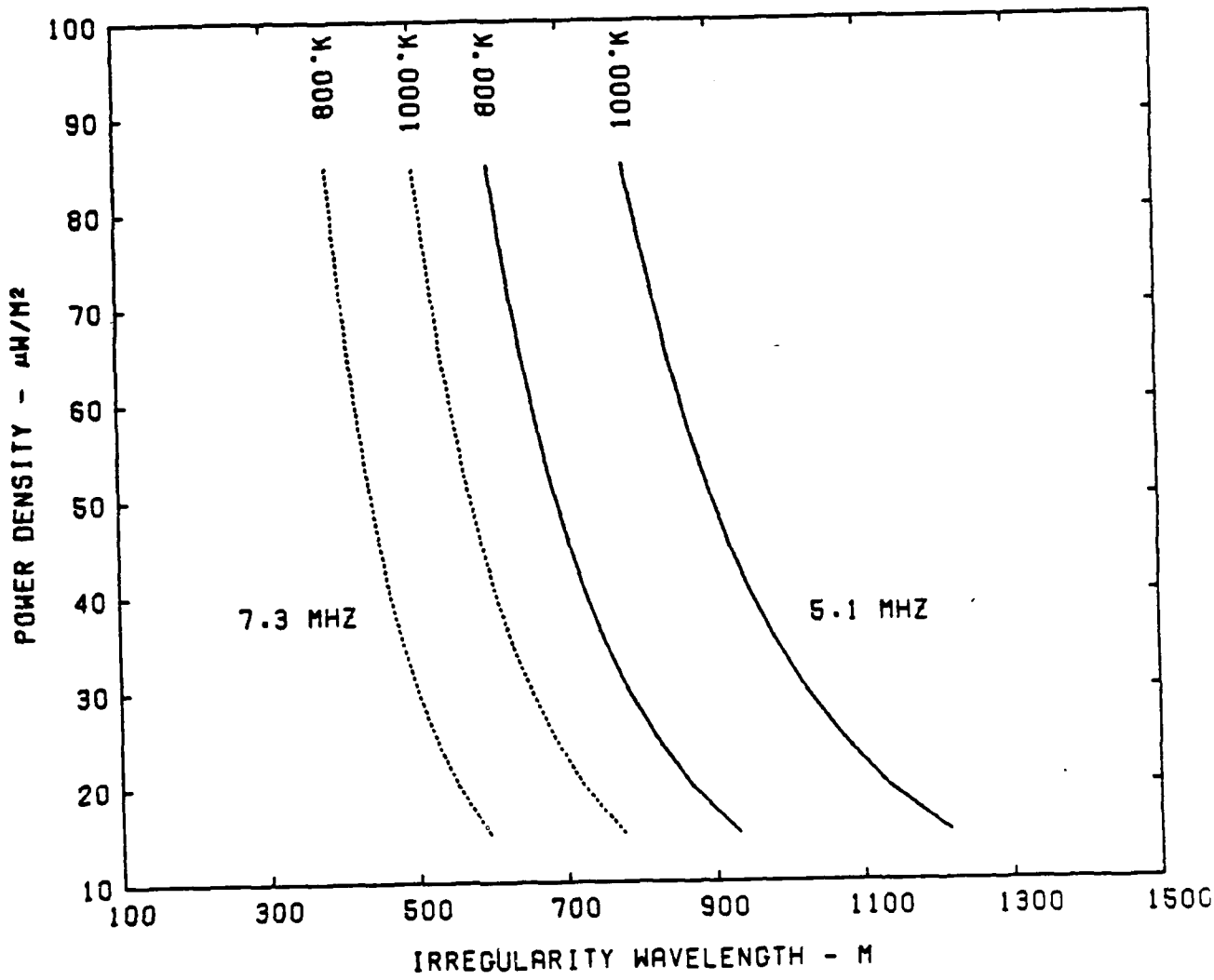

Figure 1. Thermal Self-Focusing Irregularity Wavelength Dependence on in situ HF Power Density, after Cragin et al. (1977). The heating frequencies of 5.1 MHz (solid) and 7.3 MHz (broken) are those used in the experiment. The assumed plasma scale height is 100 km, and the background electron-ion temperatures are as indicated.

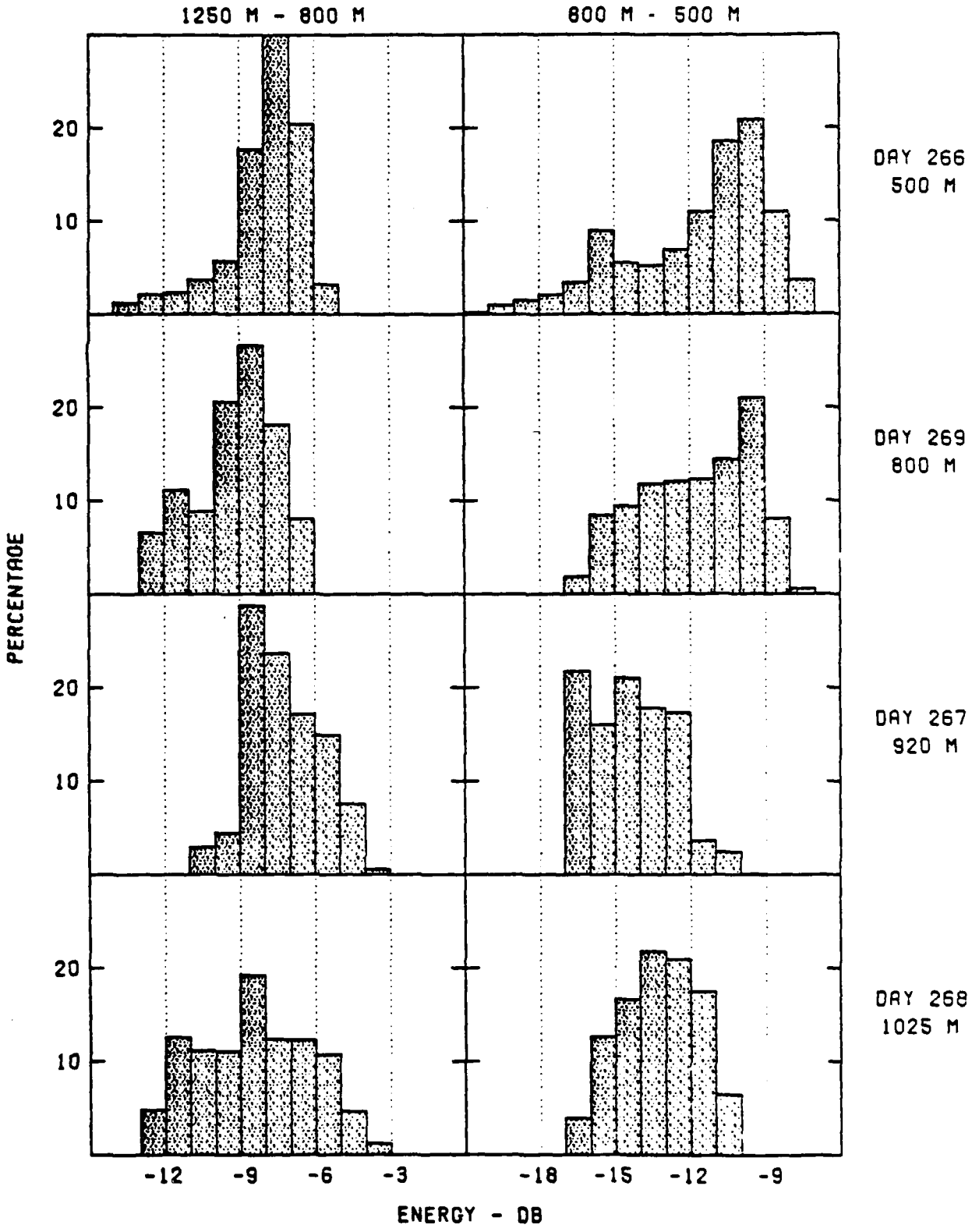

Figure 2. Distributions of Phase Energy from two Wavelength Windows for the Four Evenings of Observation. The predicted dominant self-focusing wavelength for each evening is as indicated.

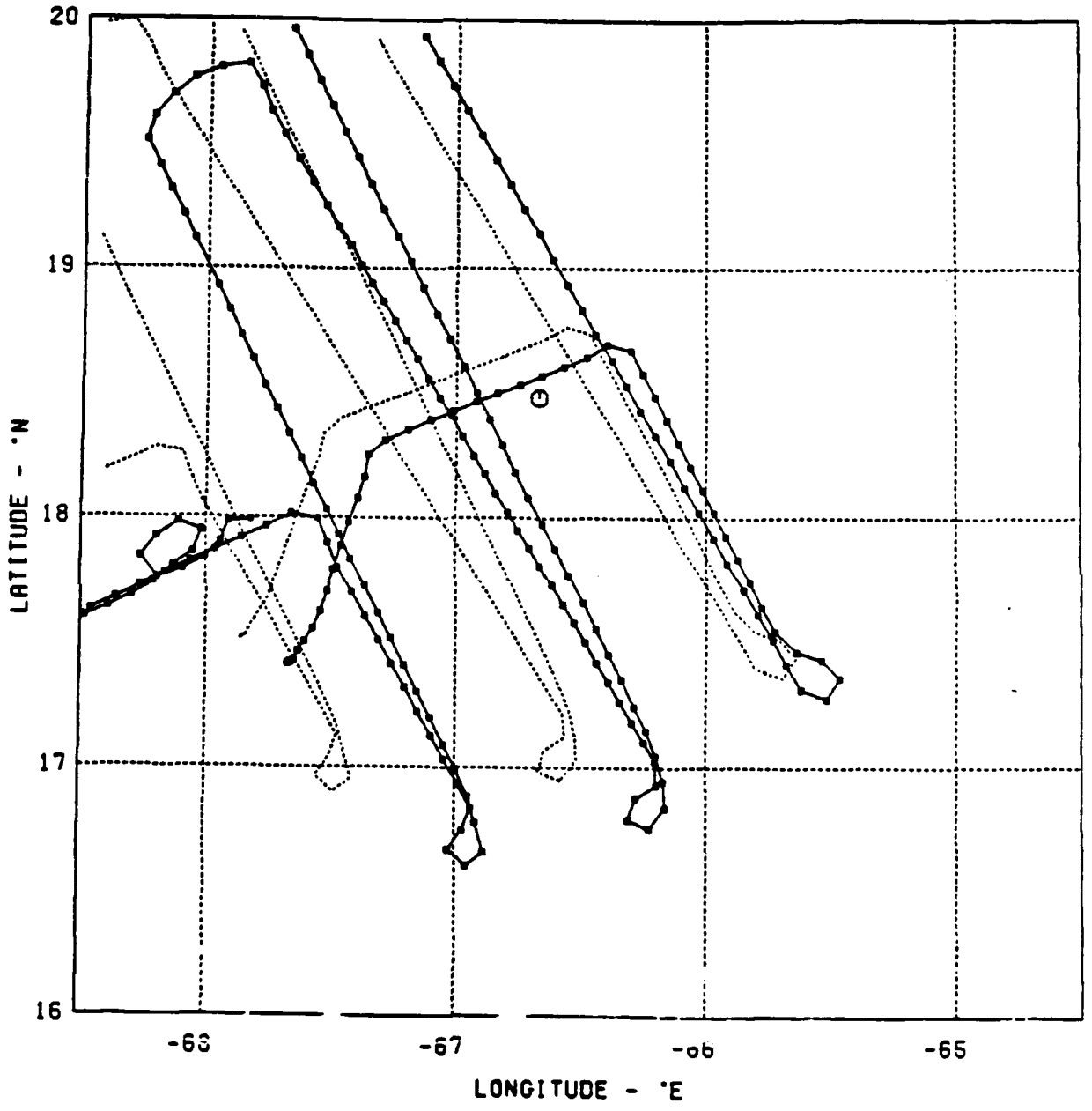

Figure 3. Propagation Raypath Penetration Locations for Day 266, 1981, for the Heating Altitude (solid) and the F Layer Peak Field Line Mapped to the Heating Latitude (broken).

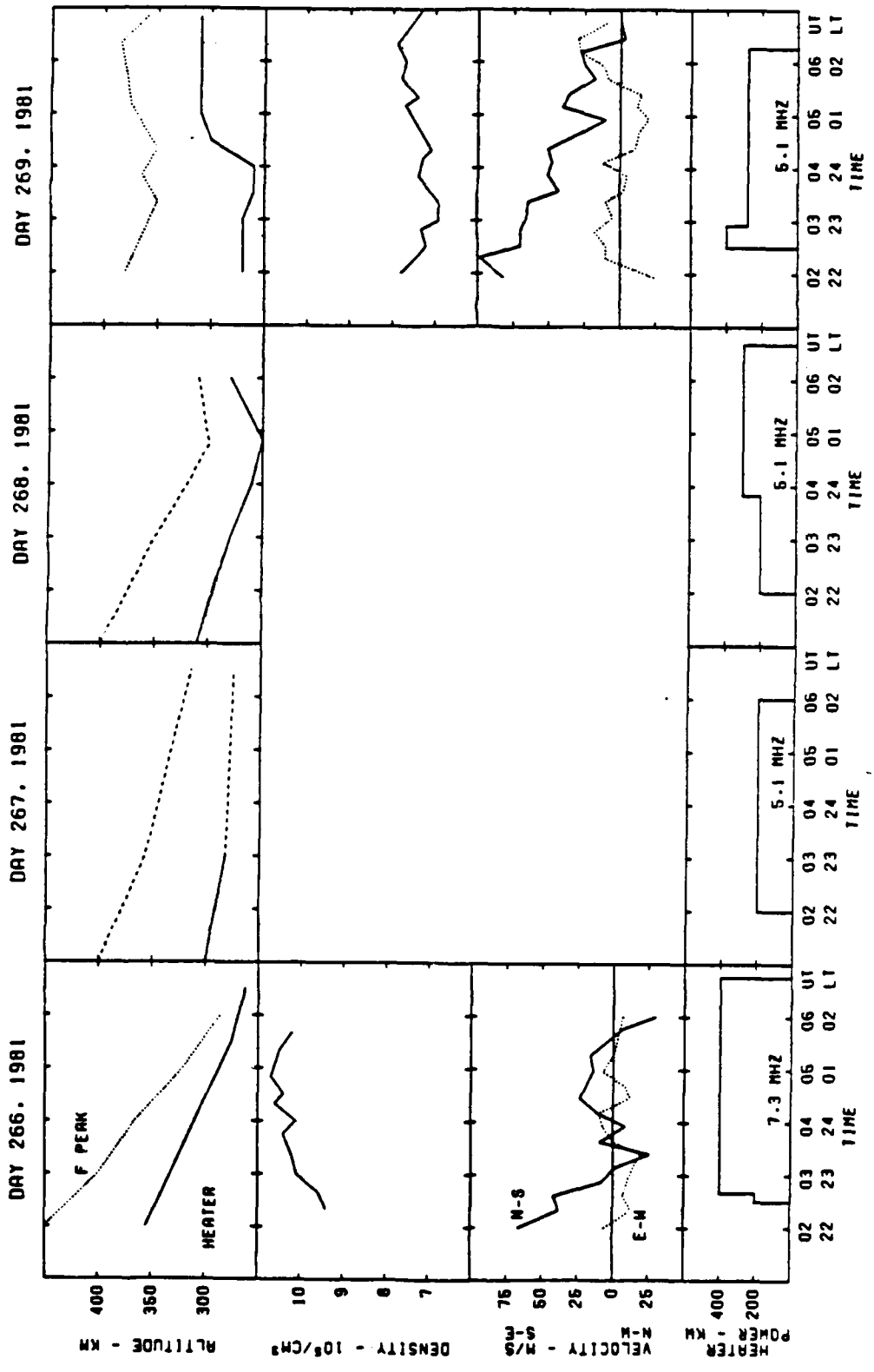

Figure 4. A Summary of Ionospheric Conditions and the Heating Schedule for the Four Evenings of Observation, Day 266 (a), Day 267 (b), Day 268 (c), and Day 269 (d). The dashed altitude lines on days 267 and 268 are estimated only.

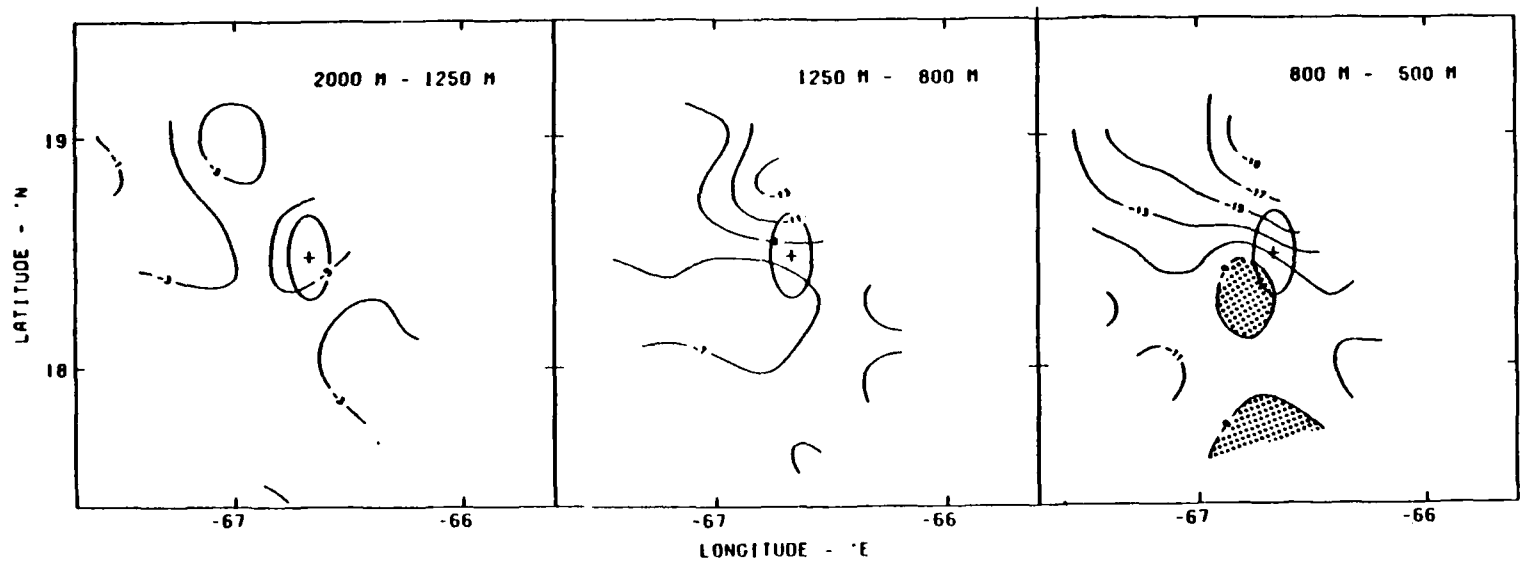

Figure 5. Phase Energy Contour Maps for Day 266, 1981, for Three Irregularity Wavelength Windows. The plus sign is the heater location, and the ellipse is the nominal 3 dB heater antenna pattern.

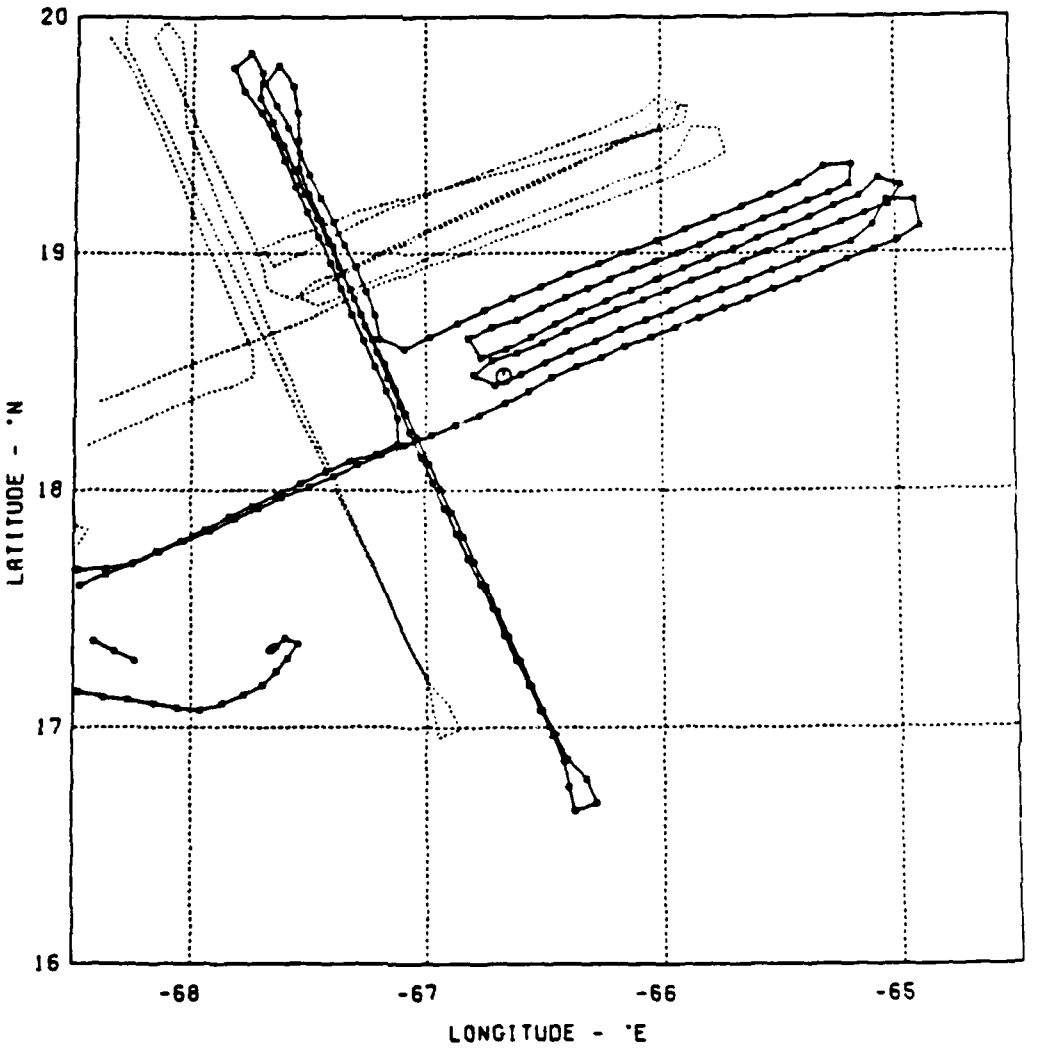

Figure 6. Propagation Raypath Penetration Locations for Day 269, 1981, for the Heating Altitude (solid) and the F Layer Peak Field Line Mapped to the Heating Altitude (broken).

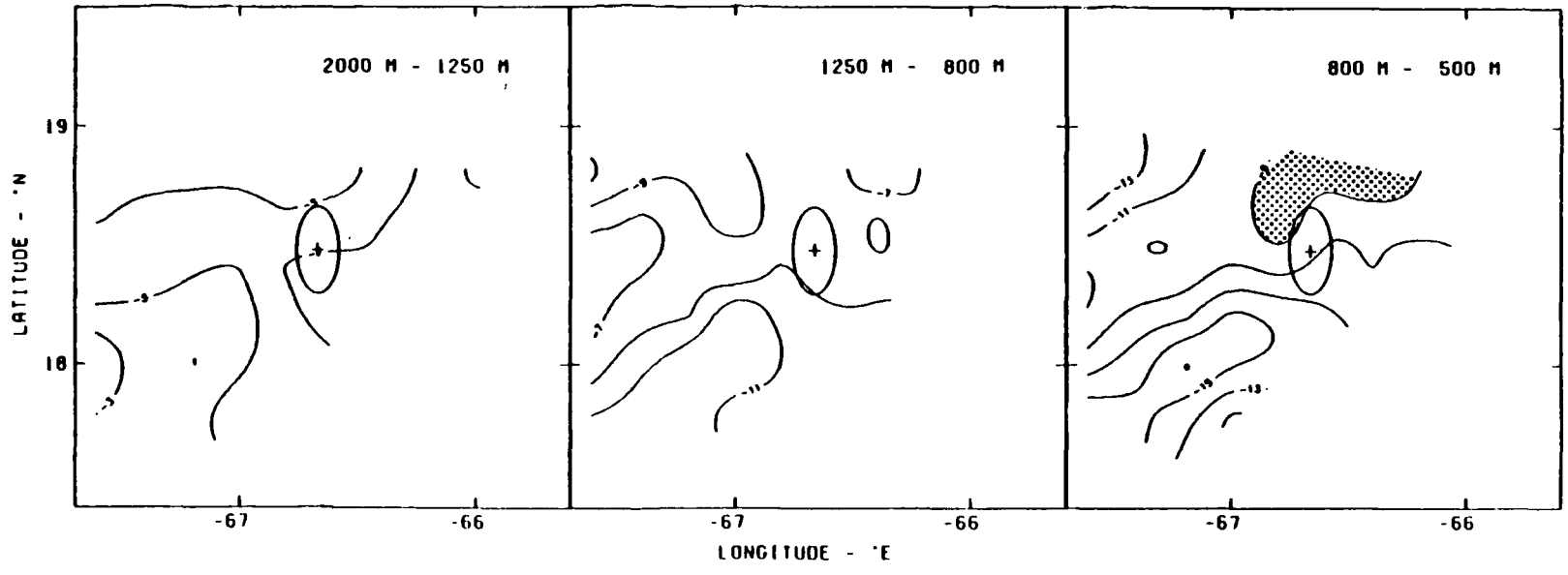

Figure 7. Phase Energy Contour Maps for Day 269, 1981, for Three Irregularity Wavelength Windows.

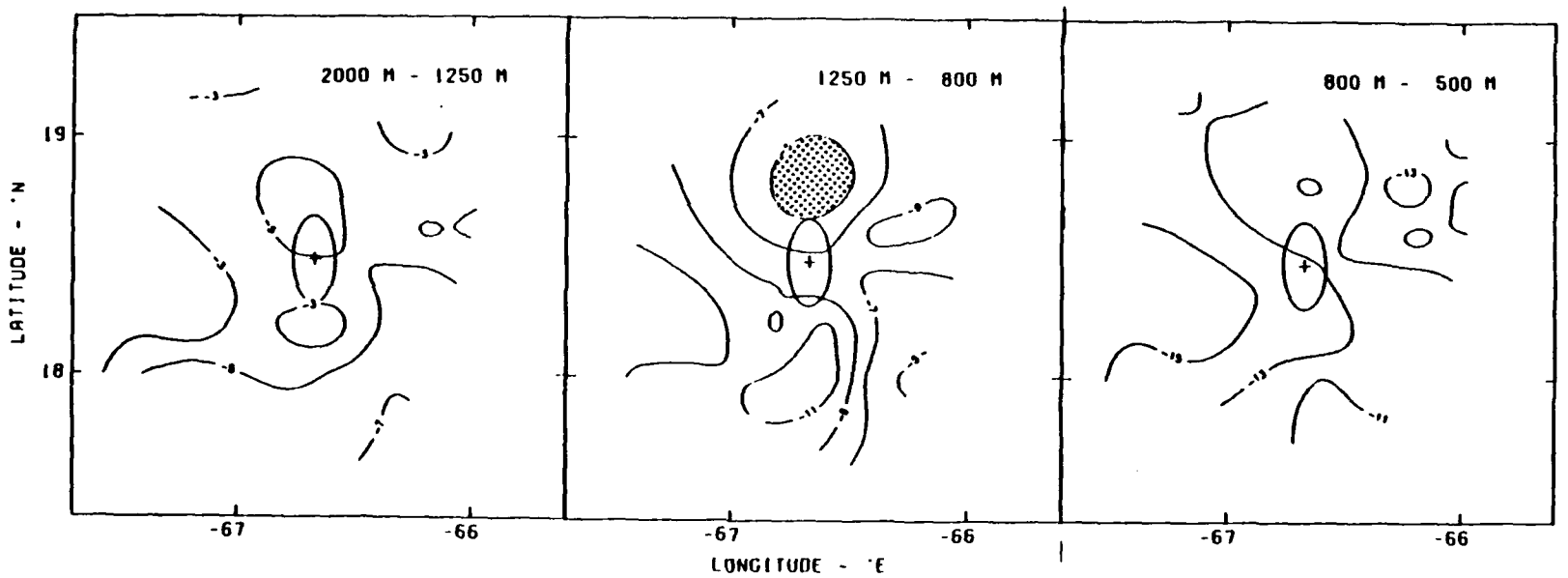

Figure 8. Phase Energy Contour Maps for Day 268, 1981, for Three Irregularity Wavelength Windows.

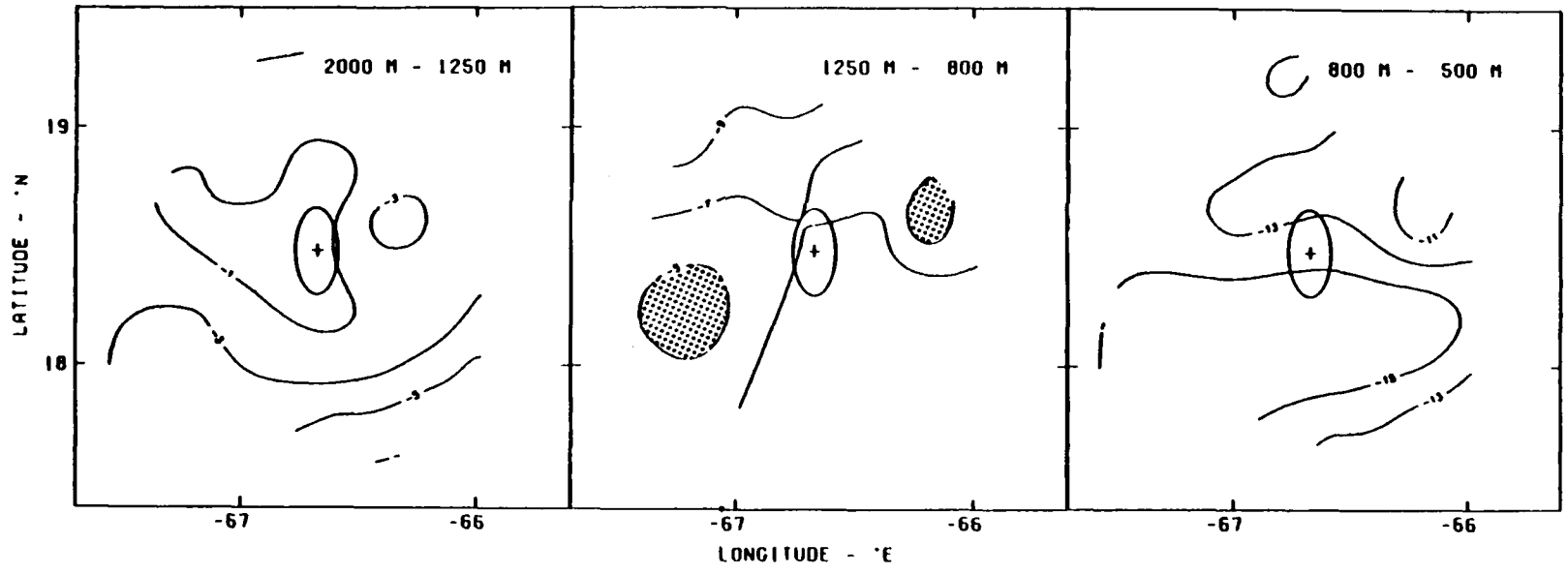

Figure 9. Phase Energy Contour Maps for Day 267, 1981, for Three Irregularity Wavelength Windows.